NEUTRON DECAY FROM GIANT RESONANCES AND THE ISOBARIC ANALOG STATE IN ^{120}Sb POPULATED IN ^{120}Sn(^{3}He,t)^{120}Sb(n)^{119}Sb CHARGE EXCHANGE

K. Ashktorab, F.D. Becchetti, J. Jänecke and A. Nadasen, D. Roberts
University of Michigan, Ann Arbor, MI 48109

G.P.A. Berg, J. Lisantti, T. Rinckel, E.J. Stephenson and S. Wells
Indiana University Cyclotron Facility, Bloomington, IN 47408

M.N. Harakeh
Natuurkundig Laboratorium, Vrije Universiteit, Amsterdam, The Netherlands

S.Y. van der Werf
Kernfysisch Versneller Instituut, Groningen, The Netherlands

S. Shaheen
King Abdul-Aziz University, Jeddah, Saudi Arabia

Figure 1 displays triton spectra for the (^{3}He,t) charge-exchange reaction measured with the K600 magnetic spectrometer and a ^{120}Sn target at $E_{^3He}$=200 MeV and angles near $\Theta = 0°$. Two different momentum bytes taken with two different K600 magnet settings extend the data to excitation energies of close to E_x=50 MeV. The ray-tracing capabilities of the focal-plane detector made it possible to decompose the observed spectra (top) into spectra centered at $\Theta = 0°$ (middle) and $\Theta = 2°$ (bottom). Residing on the non-resonant background from quasi-free charge exchange on bound neutrons (solid curve), the spectra display transitions to the 1^+ ground and other low-excited states, a very strong transition to the 0^+ isobaric analog state (IAS) at E_x=10.2 MeV with a pronounced maximum at $\Theta = 0°$, a fragmented Gamow-Teller resonance with maxima at $\Theta = 0°$, and the $T^<$ component of the charge-exchange giant electric dipole resonance with a minimum at $\Theta = 0°$. The rise in non-resonant background above $E_x = 35$ MeV, particularaly at $\Theta = 0°$, is from the breakup/pickup reaction. It can also be quantitatively described.

An important extension of the above measurements includes the simultaneous detection of evaporation neutrons from the decay of excited states and resonances. This will make it possible to extract partial decay widths including isospin-violating decays. It is also expected to enhance the observation of weak giant resonances because non-resonant background, in particular from breakup/pickup, is expected to be reduced.

Coincidence measurements with evaporation neutrons were perfected during preceeding test runs, and the performance of neutron detectors was successfully tested. The setup used during the present experiment consisted of 6 neutron detectors (4 times 2 in×2 in NE230 and 2 times 5 in×5 in Ne213) mounted at distances of 10 cm and and 30 cm from the target, respectively, in the backward hemisphere. Combining the measured neutron detection efficiency and the solid angle resulted in a total detection efficiency of 1-2%. An effective neutron/gamma ray discrimination was achieved by using pulse shape discrimination combined with time-of-flight. The latter is very useful for slow neutrons despite the short flight path. Special attention was given to achieving a low pulse height threshold

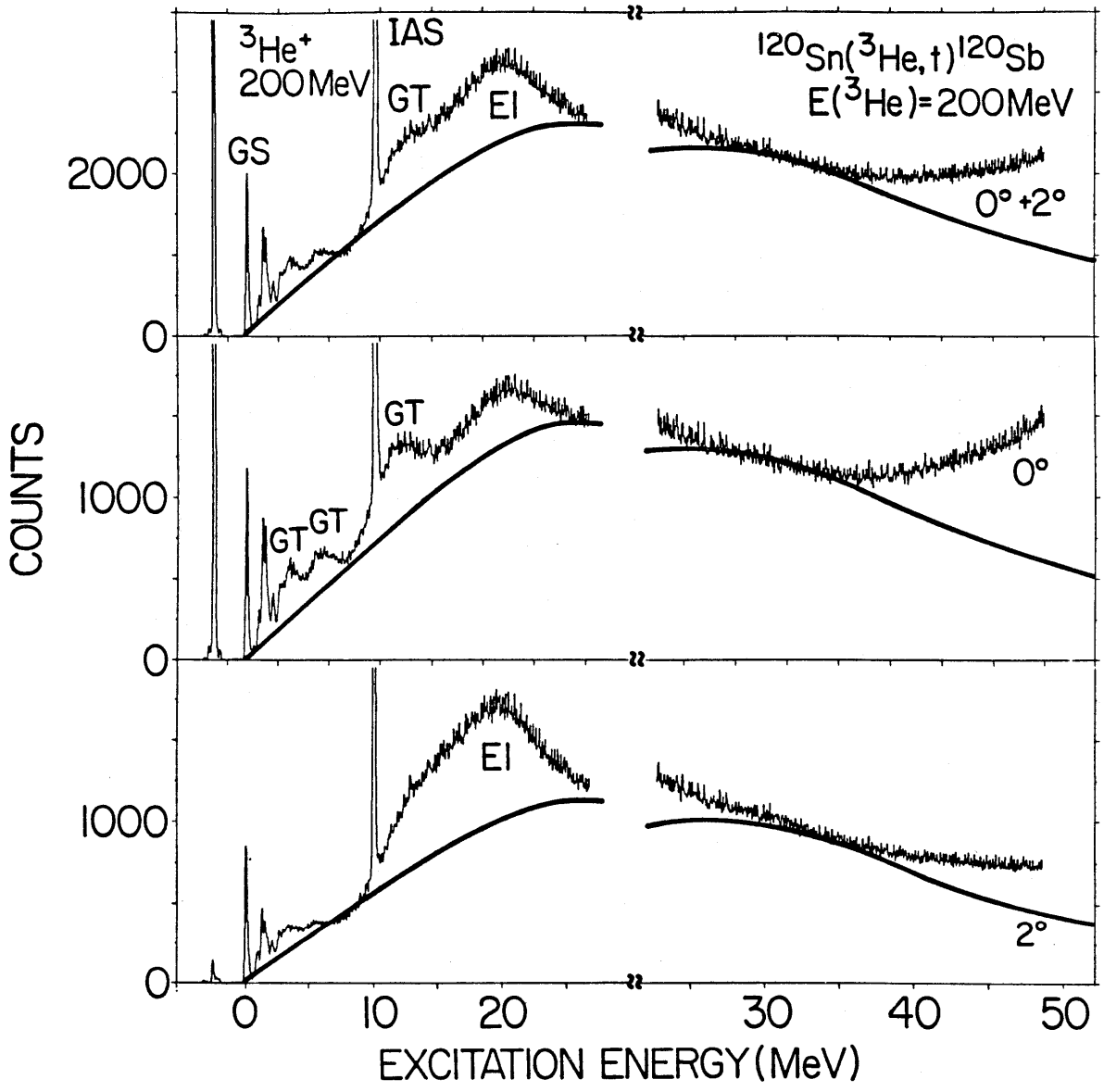

Figure 1. Triton energy spectra from the ^{120}Sn(^{3}He,t)^{120}Sb charge exchange reactions at $E_{^3He} = 200$ MeV and Θ near 0° for excitation energies up to $E_x = 48$ MeV. The middle and lower spectra represent the decomposition into components centered at $\Theta = 0°$ and $\Theta = 2°$. The spectra were obtained in two overlapping exposures.

because the emitted neutrons have low energies with a maximum of the evaporation spectrum below 1 MeV. A theshold of 30 keV electron equivalent was achieved for all detectors. This is equivalent to a neutron threshold of $\leq$ 0.5 MeV.

Figure 2 displays a preliminary triton spectrum for the low-excitation region observed in coincidence with decay neutrons. The spectrum was obtained as difference of prompt minus random (about 30%) events in the time-of-flight spectrum, but the decomposition into $\Theta = 0°$ and $\Theta = 2°$ components has not been performed yet. Also, background suppression using triton time-of-flight has not been optimized yet. Nevertheless, the figure clearly shows the onset of neutron emission at $E_x = 7.0$ MeV. The neutron decay of the IAS and the Gamow-Teller and electric dipole resonances are also seen. Non-resonant background from quasi-free charge exchange is still present, but its relative intensity is reduced by a factor of about 2.

The yield of evaporation neutrons from the decay of the IAS can be used to directly extract the branching ratio for the isospin-violating neutron decay and hence the spreading width $\Gamma_\downarrow$. Very few such data exist, and spreading widths are almost exclusively deduced indirectly from the isospin-allowed proton decay.

Using the calculated shape of the neutron evaporation spectra from the code CASCADE, the estimated and measured efficiencies for the detection of neutrons, and the observed yields, a branching ratio of close to 100% (preliminary) is obtained for the isospin-violating neutron decay.

Additional data were obtained for the region of excitation energies from 20–45 MeV with about 3 times better statistics. This includes the region of the expected giant isovector monopole resonance. The data reduction is in progress.

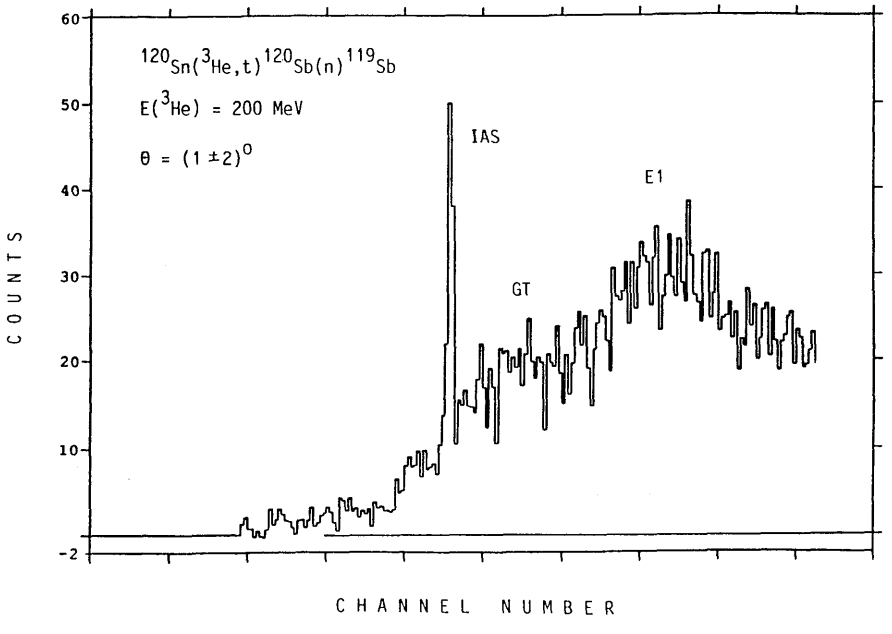

Figure 2. Triton energy spectrum from the ^{120}Sn(^{3}He,t)^{120}Sb(n)^{119}Sb charge exchange reaction at $E_{^3He} = 200$ MeV and Θ near 0° for excitation energies up to $E_x = 25$ MeV measured in coincidence with evaporation neutrons.